Research Article | Vol. 8, No. 11 | 1 Nov 2017 | BIOMEDICAL OPTICS EXPRESS 5342
Biomedical Optics EXPRESS

Measuring blood oxygen saturation along a capillary vessel in human

KFIR AKONS, ELDAD J. DANN, AND DVIR YELIN*

Faculty of Biomedical Engineering, Technion — Israel Institute of Technology, Haifa 3200003, Israel
**yelin@bm.technion.ac.il*

Abstract: Measuring oxygen saturation in capillary vessels could provide valuable information on oxygen transport and tissue viability. Most spectroscopic measurement techniques, however, lack the spatial resolution to account for the small vessel dimensions within a scattering tissue and the steep gradients of oxygen saturation levels. Here, we developed a noninvasive technique for image-guided confocal measurement of the optical absorption spectrum from a small region that is comparable in size to the cross section of a single capillary vessel. A wide range of oxygen saturation levels were measured in a single capillary in a human volunteer, with blood deoxygenation rates of 7.1% per hundred microns. The technique could help in studying oxygen exchange dynamics in tissues and could play a key role in future clinical diagnosis and therapeutic applications that require localized functional tissue inspection.

OCIS codes: (170.1460) Blood gas monitoring; (300.6460) Spectroscopy, saturation; (280.1415) Biological sensing and sensors.

References and links

1. A. C. Guyton and J. E. Hall, *Textbook of Medical Physiology* (Elsevier, 2010).
2. C. A. Lewis, W. Fergusson, T. Eaton, I. Zeng, and J. Kolbe, "Isolated nocturnal desaturation in COPD: prevalence and impact on quality of life and sleep," Thorax **64**(2), 133–138 (2009).
3. W. W. Flemons, D. Buysse, S. Redline, A. Oack, K. Strohl, J. Wheatley, T. Young, N. Douglas, P. Levy, W. McNicolas, J. Fleetham, D. White, W. Schmidt-Nowarra, D. Carley, and J. Romaniuk, "Sleep-related breathing disorders in adults: recommendations for syndrome definition and measurement techniques in clinical research. The Report of an American Academy of Sleep Medicine Task Force," Sleep **22**(5), 667–689 (1999).
4. D. D. Van Slyke and J. M. Neill, "The determination of gases in blood and other solutions by vacuum extraction and manometric measurement," J. Biol. Chem. **61**, 523–573 (1924).
5. I. Yoshiya, Y. Shimada, and K. Tanaka, "Spectrophotometric monitoring of arterial oxygen saturation in the fingertip," Med. Biol. Eng. Comput. **18**(1), 27–32 (1980).
6. G. A. Millikan, "The Oximeter, an Instrument for Measuring Continuously the Oxygen Saturation of Arterial Blood in Man," Rev. Sci. Instrum. **13**, 434–444 (1942).
7. L. Dexter, F. W. Haynes, C. S. Burwell, E. C. Eppinger, R. E. Seibel, and J. M. Evans, "Studies of congenital heart disease. I. Technique of venous catheterization as a diagnostic procedure," J. Clin. Invest. **26**, 547–553 (1947).
8. Z. D. Walton, P. A. Kyriacou, D. G. Silverman, and K. H. Shelley, "Measuring venous oxygenation using the photoplethysmograph waveform," J. Clin. Monit. Comput. **24**(4), 295–303 (2010).
9. R. H. Thiele, J. M. Tucker-Schwartz, Y. Lu, G. T. Gillies, and M. E. Durieux, "Transcutaneous regional venous oximetry: a feasibility study," Anesth. Analg. **112**(6), 1353–1357 (2011).
10. G. Hanna, A. Fontanella, G. Palmer, S. Shan, D. R. Radiloff, Y. Zhao, D. Irwin, K. Hamilton, A. Boico, C. A. Piantadosi, G. Blueschke, M. Dewhirst, T. McMahon, and T. Schroeder, "Automated measurement of blood flow velocity and direction and hemoglobin oxygen saturation in the rat lung using intravital microscopy," Am. J. Physiol. Lung Cell. Mol. Physiol. **304**(2), L86–L91 (2013).
11. B. Styp-Rekowska, N. M. Disassa, B. Reglin, L. Ulm, H. Kuppe, T. W. Secomb, and A. R. Pries, "An Imaging Spectroscopy Approach for Measurement of Oxygen Saturation and Hematocrit During Intravital Microscopy," Microcirculation **14**(3), 207–221 (2007).
12. J. Xia, A. Danielli, Y. Liu, L. Wang, K. Maslov, and L. V. Wang, "Calibration-free quantification of absolute oxygen saturation based on the dynamics of photoacoustic signals," Opt. Lett. **38**(15), 2800–2803 (2013).
13. J. Xia, J. Yao, and L. V. Wang, "Photoacoustic tomography: principles and advances," Electromagn Waves (Camb) **147**, 1–22 (2014).
14. J. B. Hickam and R. Frayser, "Studies of the retinal circulation in man: Observations on vessel diameter, arteriovenous oxygen difference, and mean circulation time," Arch. Intern. Med. **127**, 688–702 (1971).

#303210 https://doi.org/10.1364/BOE.8.005342
Journal © 2017 Received 26 Jul 2017; revised 27 Sep 2017; accepted 27 Sep 2017; published 30 Oct 2017

Biomedical Optics EXPRESS

15. D. Schweitzer, M. Hammer, J. Kraft, E. Thamm, E. Königsdörffer, and J. Strobel, "In vivo measurement of the oxygen saturation of retinal vessels in healthy volunteers," IEEE Trans. Biomed. Eng. **46**(12), 1454–1465 (1999).
16. J. Lecoq, A. Parpaleix, E. Roussakis, M. Ducros, Y. Goulam Houssen, S. A. Vinogradov, and S. Charpak, "Simultaneous two-photon imaging of oxygen and blood flow in deep cerebral vessels," Nat. Med. **17**(7), 893–898 (2011).
17. A. Y. Lebedev, A. V. Cheprakov, S. Sakadzić, D. A. Boas, D. F. Wilson, and S. A. Vinogradov, "Dendritic Phosphorescent Probes for Oxygen Imaging in Biological Systems," ACS Appl. Mater. Interfaces **1**(6), 1292–1304 (2009).
18. H. Komatsu, M. Ikawa, K. Karita, and S. Fukumoto, *Measurement of Tissue Oxygenation Level in Human Lip, Interface Oral Health Science* (Springer, 2012).
19. S. Jacques and S. Prahl, "Tabulated Molar Extinction Coefficient for Hemoglobin in Water" (1998), retrieved *http://omlc.org/spectra/hemoglobin/summary.html*.
20. S. L. Jacques, "Optical properties of biological tissues: a review," Phys. Med. Biol. **58**(11), R37–R61 (2013).
21. K. P. Ivanov, M. K. Kalinina, and Levkovich YuI, "Blood flow velocity in capillaries of brain and muscles and its physiological significance," Microvasc. Res. **22**(2), 143–155 (1981).
22. M. Stücker, V. Baier, T. Reuther, K. Hoffmann, K. Kellam, and P. Altmeyer, "Capillary blood cell velocity in human skin capillaries located perpendicularly to the skin surface: measured by a new laser Doppler anemometer," Microvasc. Res. **52**(2), 188–192 (1996).
23. M. Friebel, A. Roggan, G. Müller, and M. Meinke, "Determination of optical properties of human blood in the spectral range 250 to 1100 nm using Monte Carlo simulations with hematocrit-dependent effective scattering phase functions," J. Biomed. Opt. **11**(3), 34021 (2006).

1. Introduction

The process of oxygen delivery to the tissue occurs primarily at capillary vessels, where oxygen molecules detach from the hemoglobin in the red blood cells and diffuse through the vessel walls into the tissue. Over relatively short flow paths, blood oxygen saturation drops from the typically high (>90%) arterial oxygenation levels to the low (<60%) oxygen levels, typical to venous blood [1]. In arteries, abnormal blood oxygenation levels are often associated with severe medical conditions, including hypoxia, chronic obstructive pulmonary disease [2] and obstructive sleep apnea [3]. Techniques for measuring arterial oxygen saturation levels in humans include gas analysis of extracted blood [4] or, more frequently, noninvasive measurement of the optical absorption by hemoglobin [5], a technique commonly referred to as pulse oximetry [6]. In veins, blood oxygen levels depend mainly on the consumption of oxygen by the tissue. Venous oxygen saturation is commonly measured using invasive catheterization [7] or by noninvasive methods using the photoplethysmograph waveform [8] or Fourier-domain analysis of light absorption in large veins [9]. While arterial and venous oxygenation levels could provide diagnostic information on the oxygen supplied to and consumed by large tissue regions and end organs, efforts were made to estimate local oxygen exchange for measuring tissue viability on smaller scales, using intravital microscopy [10, 11] and photoacoustic tomography [12, 13]. In the retina, where arterial and venous vessels can be easily imaged, local blood oxygenation was measured via spectroscopy of individual vessels [14, 15]. High spatial and temporal resolution measurement of oxygen saturation in thick scattering tissue was also reported in exposed brain tissue [16] and using phosphorescent probes [17]. In the human lips, average tissue oxygenation was estimated by measuring the relative optical absorption by hemoglobin and oxy-hemoglobin [18].

Measuring the oxygenation levels along a single capillary vessel within a scattering tissue is challenging not only because of the small dimensions of these vessels, but also because in contrast with arterial and venous blood, the continuous oxygen exchange between the vessel and the tissue yields saturation levels that vary considerably along relatively short paths within a single vessel. In this work, we present a novel, non-invasive and label-free technique, termed spatially incoherent confocal spectroscopy (SICS), for measuring the absorption spectrum at specific locations within individual capillary vessels in the human lip. By measuring the absorption spectra from small, well-defined tissue regions we estimate blood oxygenation within a capillary vessel and measure the rapid oxygen exchange between a capillary vessel and the surrounding tissue.

Biomedical Optics EXPRESS

2. Experiment

The optical system for measuring oxygen saturation at small regions within blood vessels employs (Fig. 1) single-point confocal measurement with a point-spread function tailored to the typical diameter of a capillary vessel. Incoherent light from a broadband laser-driven light source (Energetiq EQ.-99, 320-2200 nm) was guided by a multimode fiber (F1) with a 50 µm core diameter, collimated by a 15.4-mm-focal length aspheric lens (L1), bandpass filtered (BP, 500-680 nm), and focused by an objective lens (L2, NA = 0.75, × 20, Nikon) onto a small region in the inner lower lip of a healthy volunteer. The illuminated area, illustrated as a large oval in Fig. 1(a) (inset), covered an approximately 33 µm diameter spot (calculated assuming × 0.66 demagnification) inside the tissue, resulting in maximum irradiance of approximately 1.6 W/cm^2 at the focal plane. For controlling the exact measurement location, the volunteer's lip was positioned in contact with a 170-µm-thick cover glass glued to an aluminum cup that was mounted on a three-axis manual translation stage. Maneuvering the aluminum cap (and hence the tissue in contact) by the translation stage allowed adjustment of the field of view with respect to the (static) objective lens. Backscattered light from the tissue was deflected by a non-polarizing beam-splitter (BS), coupled by an achromatic lens (L3, 50 mm focal length) into an optical fiber with 11 µm core diameter, and analyzed by a custom-built spectrometer comprised of a collimating lens (50 mm focal length), a transmission diffraction grating (1700 lines/mm), a focusing lens (50 mm focal length) and an electron-multiplying CCD camera (Andor, Newton DU970N-BV). The collection core diameter (11 µm) and the × 0.2 demagnification collection optics resulted in an effective collection region (small oval in Fig. 1(a) inset) with a diameter of approximately 2.2 µm. The resulting confocal point-spread function (Fig. 1(b)) was approximately 30 µm wide (FWHM) and 42 µm deep (FWHM), measured by translating a mirror and a reflective edge across the focal volume. Spectral acquisition rate and resolution were 10 spectra/s and 0.17 nm, respectively.

The measurement area within the lip was illuminated using a narrow-band blue LED (Thorlabs M455-F1, 455 nm central wavelength), a 20-mm focal length collimating lens (L4) and a long-pass dichroic mirror (DM1, 490 nm cutoff wavelength), and imaged by a similar dichroic mirror (DM2), an achromatic lens (L5) and a monochrome CCD camera (IDS UI-2220SE, 25 Hz). Due to the high absorption of the blue wavelength by hemoglobin, blood vessels appeared dark in the widefield image, with a bright diffusive background light emanating from the tissue. A pair of crossed linear polarizers (LP) was used to reduce glare and surface reflections. Data from the spectrometer and from the camera was sampled and displayed in real-time using custom-built software (Labview, National Instruments), and stored on the computer hard-drive.

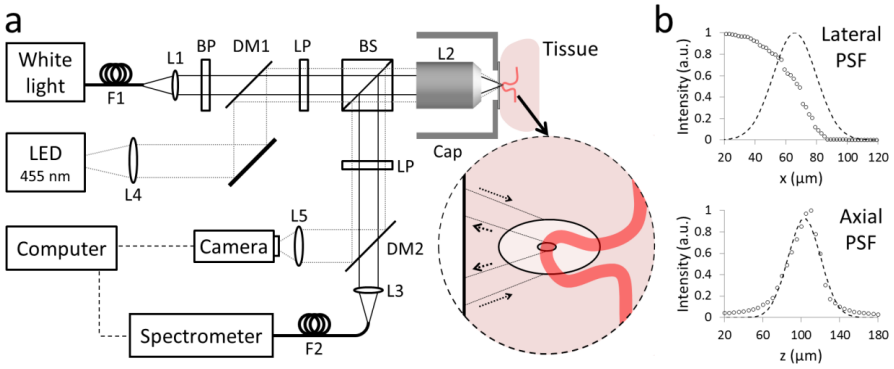

Fig. 1. (a) Schematic illustration of the optical setup for spatially incoherent confocal point spectroscopy. L1..L4 – Achromatic lenses. BP – bandpass filter. LP – linear polarizer. DM1, DM2 – dichroic mirrors. (b) Lateral and axial cross-sections of the measured point-spread function (PSF). Circles – total reflection measurement. Dashed curve – best fit to a Gaussian function.

Biomedical Optics EXPRESS

For *in vivo* measurement of local blood oxygen saturation in capillary vessels, a healthy volunteer (male, age 29) placed his chin on a padded chin rest and positioned his lower lip against the cover glass. Due to the typically thin epidermis and absence of melanin in the oral mucosa, capillary vessels at the inner lower lip were easily visible on the widefield camera image (Fig. 2(a)). A 20-µm-thick vessel identified approximately 100 µm below the tissue surface was maneuvered using the three-axis translation stage into the measurement point located at the center of the field of view. Reflection spectra measured from points 1-6 marked in Fig. 2(a) revealed (Fig. 2(b)) the characteristic absorption of hemoglobin [19] with minima at approximately 542 nm and 576 nm. Each spectrum (100 ms exposure time) was smoothed using a moving average filter (0.85 nm, 5 pixels). Note that the reflection spectrum from point 4 (Fig. 2(a), bold curve) located on the vessel was considerably lower compared to spectra from points more distant from the vessel, and exhibits the most pronounced hemoglobin spectral features. Using the spectrum I_4 captured from point 4 on the vessel, the absorption of each wavelength λ (Fig. 2(c), solid line) was estimated using:

$$a(\lambda) = -\log_{10}\frac{I_4(\lambda)}{I_1(\lambda)}, \tag{1}$$

where I_1 denotes the spectrum from the remote point 1 that was used here as reference. Note that for a bias-free measurement, an ideal reference spectrum should not include hemoglobin absorption. Using linear regression for the wavelength range between 536 nm and 586 nm, the absorption vector $a(\lambda)$ was then fitted (Fig. 2(c), dashed red line) to a linear summation of three different principal vectors according to:

$$a(\lambda) = A + B\mu_{HbO_2}(\lambda) + C\mu_{Hb-R}(\lambda) + D\lambda^{-1.47}, \tag{2}$$

where μ_{HbO_2} and μ_{Hb-R} denote the molar extinction of fully (100%) oxygenated and deoxygenated hemoglobin, respectively, the term $D\lambda^{-1.47}$ denotes an approximate scattering coefficient of a tissue (obtained from Ref [20]), and *A*-*D* are positive fit parameters. Blood oxygen saturation for each spectrum was estimated as the ratio between oxygenated and total hemoglobin using:

$$SO_2 = \frac{B}{B+C}. \tag{3}$$

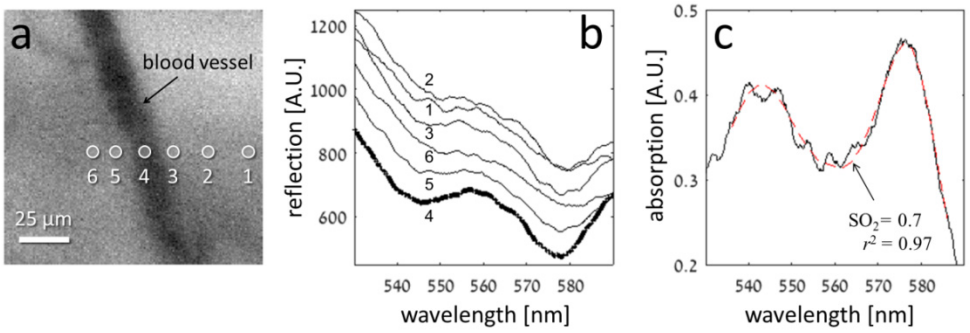

Fig. 2. (a) Widefield image of a target vessel (marked by an arrow) with six measurement locations marked by white circles. (b) Reflection spectra from the six points. Bold curve corresponds to location #4 on the vessel. (c) Absorption spectrum (black solid line) calculated using spectrum #4 with spectrum #1 as reference. Curve fit (red dashed line) resulted in estimated saturation value of 0.70 with r-squared value of 0.97.

Biomedical Optics EXPRESS

As oxygen concentration varies rapidly in small capillaries, measuring blood oxygenation at a single point would have little meaning outside the context of the entire vessel. In order to demonstrate the variability in oxygen saturation along a capillary vessel, four measurements were conducted at four different locations (Fig. 3, I-IV) along a capillary loop approximately 80 μm below the surface. Over 600 spectra were acquired from each location during four minutes total measurement time. The spectra were smoothed using a running average of ten consecutive spectra. To reduce the effect of corrupted data due to motion artifacts, spectra with integrated intensities (area under the curve) that deviate significantly from the mean value (acquired from the specific location) were excluded from the calculations, resulting in a total of 100 usable spectra from location I and 400 spectra from each of the locations II-IV. The absorption spectra were calculated from each spectrum Eq. (1) using a reference spectrum that was obtained by averaging over 20 spectra captured from randomly distributed points distant (more than 60 μm) from the blood vessels. The absorption spectral curves were then fitted to Eq. (2) and the corresponding oxygen saturation (SO_2) values for each of the points I-IV were calculated using Eq. (3). The mean oxygen saturation at each measurement point (shown at the lower-right of each plot) was calculated using only saturation values (black dots) that exhibited r-squared fit values (blue dots) within one standard deviation from the average r-squared value, or higher (threshold marked by dashed lines). Oxygen saturation values of 0.847, 0.863, 0.876 and 0.916 were measured for locations I, II, III and IV, respectively, with typical standard deviations between 0.013 and 0.04.

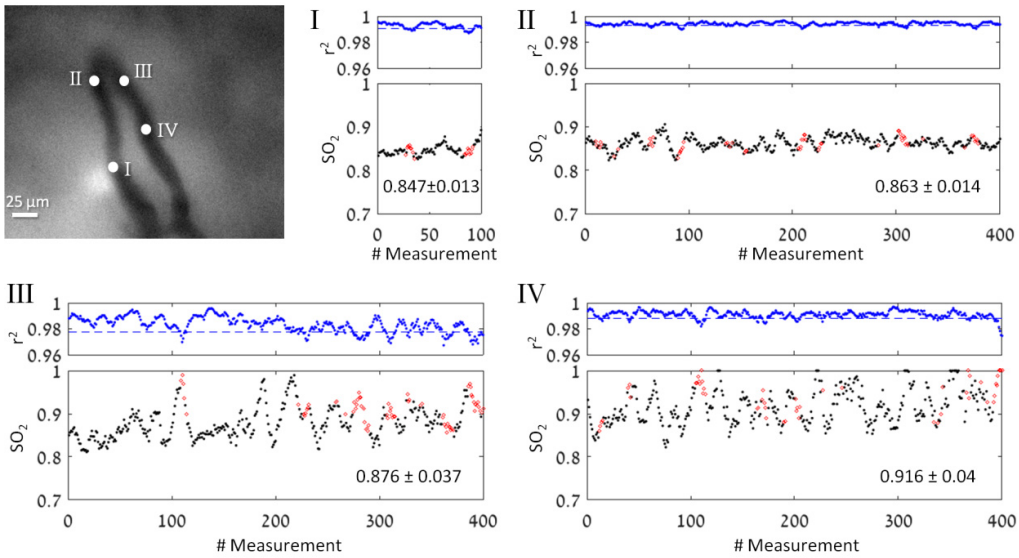

Fig. 3. Oxygen saturation measurements using SICS at four locations on a capillary loop. Top-left inset: widefield image of the target vessel. I-IV: approximate measurement locations. Plots I-IV: calculated oxygen saturation values (black dots) and the corresponding r-squared values (blue dots) for the spectra captured from each location. Dashed line in the r-squared plots denote the threshold values below which the corresponding oxygen saturation values (red dots) were excluded from the calculations.

In order to demonstrate and visualize the gradual oxygen loss from a blood vessel, oxygen saturation levels were measured along a capillary loop at seven different points uniformly distributed at approximately 40 μm intervals (Fig. 4(a)). Excluding a single measurement point (SO_2 = 0.75, bottom-right), whose location near a vessel intersection may result in averaging over multiple oxygenation levels, the saturation values, represented by a red-blue color palette, were linearly interpolated between the measured points to illustrate the gradual depletion of blood oxygen. The drop in oxygen saturation along the capillary loop agrees with the observed counterclockwise direction of the blood flow, which is shown in Visualization 1.

Biomedical Optics EXPRESS

The measured oxygen saturation levels are plotted (Fig. 4(b)) as a function of the flow path length (estimated from Fig. 4(a)), revealing significant oxygen depletion of 16% at a rate of approximately 7.1% per 100 μm. Assuming an average flow velocity of 500 μm/s [21, 22] and a typical adult hemoglobin concentration of 150 g/L, these rates correspond to approximately 1.4×10^{11} oxygen molecules transferred to the tissue every second from a 100 μm segment of the vessel.

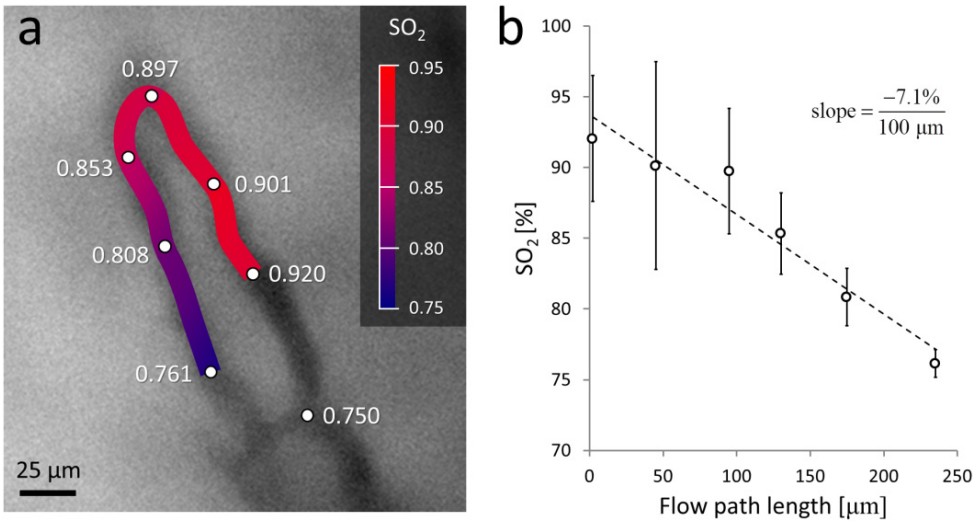

Fig. 4. Blood oxygen loss from a capillary loop. (a) Oxygen saturation values interpolated between six measurement points. (b) Measured saturation level as function of blood flow path length. Error bars represent standard deviations. Linear curve fit (dashed line) indicate average oxygen saturation loss of 7.1% per 100 μm.

3. Discussion

Measuring oxygen saturation in capillary vessels with high spatial resolution is valuable for studying oxygen transport from the blood to the tissue on small scales and for assessing local tissue viability, for example within damaged or transplanted/engineered tissue. The rapid blood flow through the complex network of small vessels embedded within a highly scattering tissue, however, presents numerous challenges for optical sensing techniques, including high scattering by the blood cells, low absorption coefficients in the near-infrared range, and the characteristic strong spatial gradients of oxygen saturation levels within the blood. Advanced high-resolution spectral imaging approaches including intravital microscopy [11] and photoacoustic tomography [12] are suitable for measuring blood oxygenation is large networks of small vessels; in comparison, SICS is considerably simpler and is suitable for measurement at small regions of interest in a highly-scattering tissue. Our approach for addressing these challenges combined several techniques for optical point-spread function design, data acquisition and data analysis. First, instead of the near-infrared light commonly used for diffused optical sensing, we used light at the visible range of the spectrum due to its high absorption by blood; the hemoglobin absorption coefficients at 530 nm is approximately 21.4 mm^{-1} [19, 23], resulting in over 20% of the light absorbed within a 10-μm-thick vessel. For comparison, less than 1% of 800 nm light (0.4 mm^{-1} hemoglobin absorption coefficient) would be absorbed in similar size vessels. Second, SICS uses large fiber cores for light delivery in order to maintain low speckle noise (approximately 1%) and to improve signal-to-noise ratio in the recorded reflection spectra; using a smaller core fiber (5 μm, single-mode) instead of the current collection fiber (11 μm core diameter) improved the resolution by 1.5-fold, but resulted in approximately 6-fold increase in speckle noise and 4-fold decrease in signal. Using large illuminated volumes also allowed SICS to achieve low irradiance levels

Biomedical Optics EXPRESS

for avoiding tissue damage; this configuration is particularly suitable for spatially incoherent illumination sources (such as the laser-driven light source used for this work). Third, capturing an entire spectrum is known to be advantageous over measurements at discrete wavelength [5], as curve-fitting algorithms rely on a considerably larger sample size that results in lower error-of-estimate of the fit parameters. Fourth, a widefield real-time imaging channel was used for keeping the measurement point on the target vessel. Such visual guidance was necessary for triggering data collection and discarding spectra captured away from the target vessel. Finally, in order to avoid washout of spectral features under the constant motion, exposure time was kept short (100 ms) while averaging was performed over individual SO_2 values that were calculated from each spectrum. The r-squared values calculated for each curve fit was used to exclude SO_2 values that resulted from unphysical spectra, i.e. spectra that deviate from the linear combination presented in Eq. (2).

Some challenges remain before SICS could be used effectively for measuring capillary oxygen levels in research and clinical applications. The high spatial resolution of the measurement requires fixed positioning of the optical system with respect to the tissue, with micron-scale adjustments of the field of view. A possible solution to this challenge may involve a soft mechanical fixture that maintains stable contact between the optics and the tissue while avoiding tissue compression that could reduce blood flow. Another difficulty encountered during our experiments was acquiring a hemoglobin-free reference spectrum for computing oxygen saturation levels without bias. Because the measurement point-spread function extends somewhat beyond its central oval region, absolute spectral measurement could be difficult in the vicinity of large blood vessels. Our approach for acquiring a reference spectrum by averaging over spectra near the target vessel may involve bias and thus be limited only to relative blood oxygenation measurements. Other approaches for obtaining a hemoglobin-free reference spectrum include using calibrated tissue phantoms and simulations of light propagation in numerical tissue models.

In summary, an optical system that allows non-invasive, label-free measurement of oxygen saturation in small capillary vessels has been demonstrated using image-guided confocal measurement of small tissue volumes. Variable oxygen saturation levels were demonstrated in single capillary vessels, and a significant oxygen loss rate of 7.1% per 100 μm was measured in a single capillary loop. The presented technique could be used to study oxygen exchange dynamics in tissues and could be useful for clinical applications that require localized tissue inspection.

Funding

The study was funded in part by the Israel Science Foundation grant (651/14). This work was also supported in part by the Lorry I. Lokey Interdisciplinary Center for Life Sciences and Engineering.

Disclosures

The authors declare that there are no conflicts of interest related to this article.